KLA INSTRUMENTS

Characterization of Mechanical Deformation in Flexible Electronic Structures

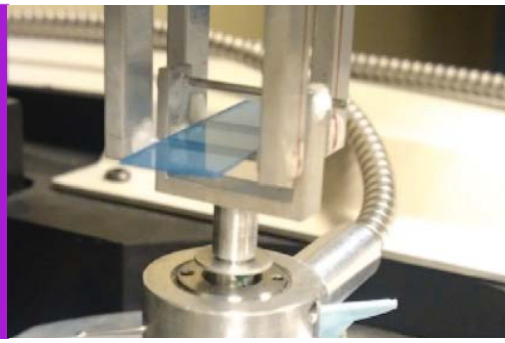

Introduction

The advent of new materials holds great promise for designing flexible electronic structures that can be used for applications such as displays, integrated circuits, light emitting diodes (LEDs), photovoltaics, biomedical devices, etc. Many of these devices rely on multilayer structures, with thin films (metallic and/or ceramic) coated on a polymer substrate. However, among several factors, the mechanical stability of the device plays an important role in determining its performance. When the different layers are subject to stress, the inorganic thin film tends to fail or plastically deform, which, in turn, degrades the performance of the device. Hence, characterization of failure stresses in multilayer structures is of great importance in the research and development process of flexible electronic devices.

Plastic deformation mechanisms in thin films differ significantly from their bulk counterparts. For bulk brittle materials, crack initiation is the dominant failure mechanism. But, in brittle thin films, failure is more dependent on crack propagation. Any material, in sufficiently thin form, is flexible because of the reduced bending strains that decrease linearly with thickness.[1] There is growing interest in the field of flexible electronics, and there have been few studies on mechanical deformation using vibration, X-ray diffraction, nanoindentation and tensile testing. However, challenges still remain to characterize the exact failure mechanisms, especially at the smaller length scales.

The main objective of this study is to determine the strength and limitations of the KLA T150 UTM, a nanomechanical tester from KLA Corporation, in characterizing the failure mechanisms in flexible electronic structures under bending. The T150 UTM is specifically designed to measure mechanical deformation of materials with small dimensions. The high accuracy in measuring force and displacement has already been utilized to characterize tensile deformation in thin fibers.[2-7] Moreover, the T150 UTM can be operated in three point bending mode, which makes it suitable for characterizing flexural failure modes in inorganic thin films on flexible substrates. The unique design of the nanomechanical actuating transducer (NMAT) is also capable of applying a harmonic force continuously to measure the dynamic elastic response of the sample. This continuous dynamic analysis (CDA) enables us to detect small changes in material structures more effectively compared to a quasi-static mechanical experiment. Therefore, it has been hypothesized that the CDA will be an effective tool to characterize the brittle failure in thin flexible electronic structures. From a broader perspective, the goal of this study is to demonstrate possible applications of the KLA nano-measurement solutions towards a better understanding of failure mechanisms in flexible electronic structures.

The following sections briefly describe the theory behind the flexural experiments, along with the dynamic analysis performed in the T150 UTM, the experimental details, results and discussion.

Theory

Bend (or Flexural) test is a commonly performed to determine the flexural stress-strain response of a material and can be used to calculate its flexural modulus. There are different geometries possible to characterize the flexural deformation of flexible electronic structures; the simplest one is 3-point bending.

The flexural stress for a sample with rectangular cross-section is given by:

$$\sigma = \frac{3PL}{2bd^2} \qquad (1)$$

where σ is the flexural stress on the outermost surface, P is the applied load, L is the length span, b is the width and d is the thickness. The corresponding flexural strain is given by:

$$\varepsilon = \frac{6Dd}{L^2} \qquad (2)$$

where ε is the flexural strain on the outermost surface and D is the maximum deflection of the center of the sample.[8]

However, these equations do not represent the actual flexural stress and strain on the thin film in the case of a bilayer material. Since the Young's moduli are different for the materials in different layers, the neutral axis of the sample shifts towards the layer of higher modulus. Consequently, the flexural properties depend on the ratio of the Young's moduli and ratio of the thickness of the film and substrate. In the case of a thin film on top of a polymer substrate, the equation for the strain on the film is given by[9]:

$$\varepsilon_{film} = \frac{d_f + d_s}{2R} * \frac{1 + 2\eta + \chi\eta^2}{[(1+\eta)(1+\chi\eta)]} \qquad (3)$$

where R is the radius of curvature, d_f and d_s are the thickness of the film and substrate, respectively. $\eta = d_f / d_s$ and $\chi = Y_f / Y_s$, where Y_f and Y_s are the Young's modulus of the film and substrate, respectively.

From simple geometry, the radius of curvature, R, can be expressed in terms of the length span, L, and the bending Deflection, D:

$$2R = \frac{4D^2 + L^2}{4D} \qquad (4)$$

Similar to the strain on film, an expression for stress on the thin film can also be formulated from the properties of both the thin film and the substrate. However, as it is not going to affect the conclusions of the current study, we considered the simple expression (Equation 1) for stress in our experiments.

There is an ISO standard test method for determining the flexural stiffness. However, the prescribed standard method is limited to quasi-static deformation of a homogeneous material. A flexible electronic structure has multiple materials and can experience larger deformation during handling. Hence, it is important to determine the changes in material stiffness with increasing deformation for a more efficient design. The continuous dynamic stiffness measurement in the T150 UTM adds the unique capability to determine the properties of the material dynamically. This is accomplished by superimposing an AC current through the coil, causing an oscillating force, F_0, on the lower grip, and the lower grip responds to this force. It oscillates with displacement amplitude z_0, and this response lags the force oscillation by a phase angle ϕ. The dynamic stiffness of the sample can be calculated as:

$$S = \left(\frac{F_0}{z_0}\right) cos\varphi \qquad (5)$$

The capability of measuring sample dynamic response continuously as a function of strain makes the T150 UTM a powerful tool to characterize the small changes in material structures and brittle failure. Thus, the dynamic stiffness measurement in the T150 UTM can ideally be used to study the cracking behavior of the thin film on top of the flexible substrate.

Experimental Details

The material used in this study is a commercial product from Sigma Aldrich (St. Louis, MO). It is a thin film of brittle ceramic Indium Tin Oxide (ITO), 100nm thick, sputter coated on a 127µm thick Polyethylene Terephthalate (PET) substrate. It has good optical transmittance (550nm, >79%) and has a surface resistivity of 60Ω/sq.[10] Samples were prepared by cutting the sheet into thin strips of required length L and width b. The size of the three point bending test block limits the maximum length of sample to 40mm and the maximum width to 20mm. However, the sample size used in this study is much smaller. The 3-point bending schematic is shown in Figure 1.

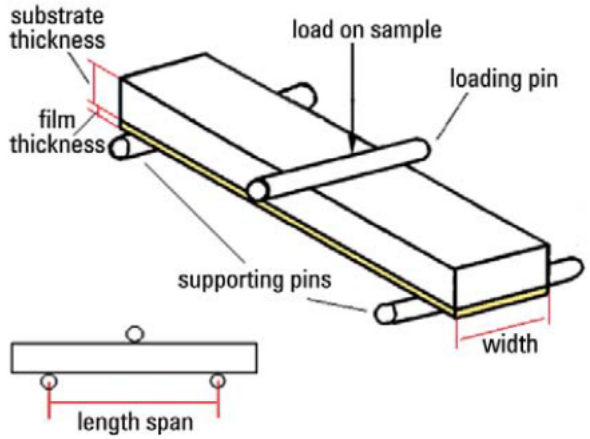

Figure 1. Schematic of a 3-point bending test setup with the film on the tensile side of bending.

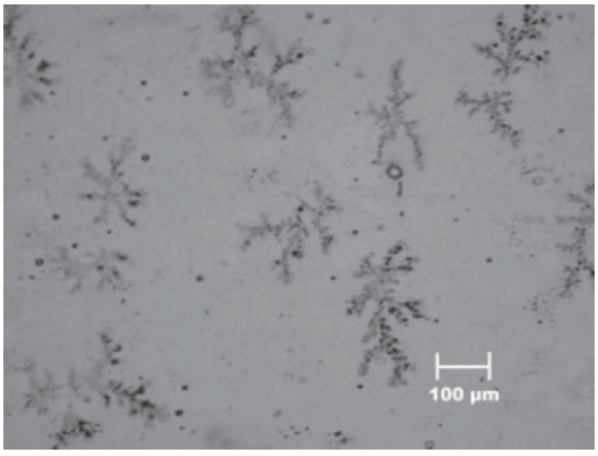

Figure 2. Optical micrograph of ITO surface showing dark spots and dendrite-like patterns.

The sample, as received, comes with a thin protective film on the ITO surface. Once this film is removed, the sample is transparent. To avoid confusion, small ink marks were made on the PET side. Optical images of the ITO surface revealed that the sample had notable surface features like dark spots and dendrite-like patterns that are uniformly distributed over the entire ITO surface, as shown in Figure 2.

The PET surface was fairly clean, with some random scratches that might have come from processing and handling. The ITO side of one sample was washed gently in deionized water and observed under the optical microscope, as shown in Figure 3. The dendrite-like patterns observed earlier, were almost completely removed, but no change was observed with the dark spots.

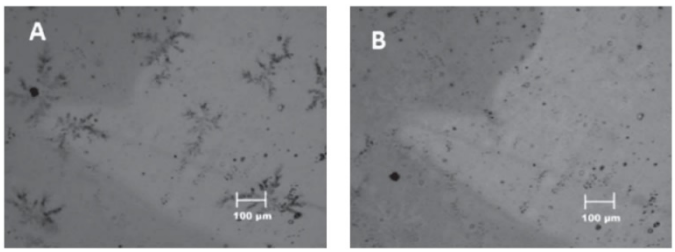

Figure 3. Optical micrograph of ITO surface (A) before water treatment, and (B) after water treatment, showing surface features removed to some extent.

Another sample was treated with ethanol for a short duration to observe any resulting change on the surface. The ethanol removed the dendrite-like patterns completely, but did remove any of the dark spots, as shown in Figures 4A and 4B. Figure 4C shows a cracked region of the ITO surface before treatment with ethanol, and, in Figure 4D, after treatment with ethanol. From the optical images it can be seen that ethanol does not alter the cracks on the ITO surface either.

Since the dendrite-like patterns were not adhered to the surface, this led us to conclude that they were residue from the protective film. As a result, the samples used in the experiments described below were carefully cleaned with ethanol prior to testing.

The Young's modulus and hardness of the thin ITO film and the PET substrate were determined using the KLA Nano Indenter® G200 with a diamond Berkovich tip. The modulus and hardness of the materials were measured with increasing displacement into the surface. The NanoSuite test method of the G200 enabled us to measure the modulus value of the thin ITO film after correcting for the substrate effect. The detailed method

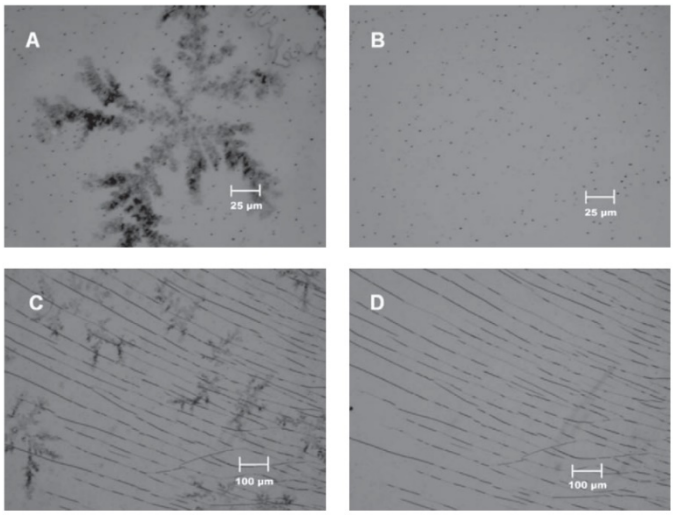

Figure 4. Optical micrograph of ITO surface, (A) before ethanol treatment; (B) after ethanol treatment, showing complete removal of dendrite like features; (C) cracked region before ethanol treatment; and (D) cracked region after ethanol treatment.

for the determination of the modulus of thin films was discussed previously in the literature.[11]

As the 3-point bending test of flexible electronic samples is a novel application for the T150 UTM, a new test method was created in NanoSuite Explorer. Along with quasi-static flexural stress and strain, the method also continuously computes the dynamic specimen stiffness during the bending test.

From Equations 1 and 2, it is evident that the flexural stress-strain measurements are sensitive to sample dimensions. Hence, at first, samples of four different dimensions (10mm x 5mm, 10mm x 3mm, 15mm x 5mm, 15mm x 3mm) were tested to select the optimum dimensions for the intended flexural study. Once the optimum dimension is established, the effect of changing deflection rates was also studied. Experiments were performed with the ITO film on the tensile side as well as the compressive side to determine the differences between the two failure modes. To ensure that our observation is related to the failure of thin ITO film, PET-only samples were prepared after completely removing the ITO film by chemical etching using 6M HCl[12] and were also characterized using the same test method.

Another modified test method was developed using NanoSuite Explorer to perform cyclic bend tests on the ITO/PET samples. The severity of cyclic testing on the samples was analyzed by taking electrical resistance measurements using a multimeter

connected to the sample with very small copper clamps across the length.

The ITO film in every sample was observed using an optical microscope (Nikon Eclipse LV150) after the test to confirm the presence of cracks. Crack morphology of selected samples was analyzed using an Agilent 8500 low voltage field emission scanning electron microscope (FE-SEM). The low voltage capability was necessary to obtain high resolution images of the cracks in the thin ITO layer. The prepared samples were fixed to a SEM stub with carbon tape and mounted onto the SEM sample stage. Imaging was performed with the slowest scan speed, with secondary electrons in normal and topographic modes, with an accelerating voltage of 1kV. The working distance varied from 1.9mm to 2.2mm.

Results and Discussion

A typical flexural load-deflection curve obtained from the 3-point bend experiment is shown in Figure 5. The deformation shows three distinct regimes marked by dashed vertical lines. In regime I, there is a linear increase in load with increasing strain. Regime II shows a deviation from linearity, which is most likely due to the viscoelastic deformation of the flexible PET substrate. At much higher deflections, the sample starts to slip from the two supports of the 3-point bend fixture, resulting in a drop in load in regime III. Hence, in the following results, the point of maximum load is decided to be the maximum deflection attainable on the current experimental setup. In other words, we only concentrate on regimes I and II for the experiments discussed below.

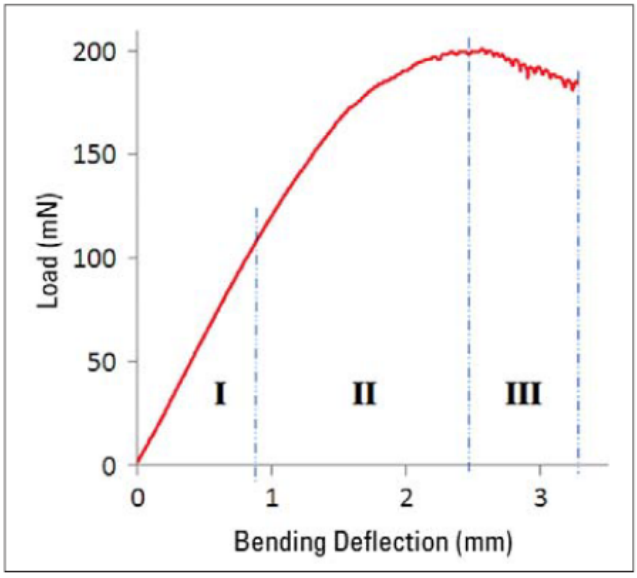

Figure 5. Typical flexural load-deflection curve obtained from the 3-point bend experiment.

The Young's modulus and the hardness values for the ITO film and PET substrate, as determined from nanoindentation, are listed in Table 1. The plot of Young's modulus with increasing depth for the ITO film and the PET substrate are shown in Figure 6. The initial low modulus in Figure 6A is most likely due to the uncertainty of tip shape calibration at very small depths. Hence, the modulus of the ITO film was estimated from depths beyond 35nm, where the modulus becomes almost independent of increasing displacement. Similarly, the modulus of the PET is estimated from a depth beyond 200nm. As the PET was 127µm thick, there was no substrate effect. From Table 1, it is clearly evident that the soft PET substrate significantly affects the measured apparent modulus on the ITO film. This is most likely the reason behind the low value of previously reported modulus for ITO film on a PET substrate.[13] Hence, the substrate effect correction is extremely crucial for modulus determination of thin films in flexible electronics.

Table 1. Young's modulus and hardness values for the ITO film and PET substrate, determined from nanoindentation experiment.

Materials	Young's Modulus (GPa)		Hardness (GPa)
	Before substrate correction	After substrate correction	
ITO film	6.0 ± 0.2	63 ± 4	0.80 ± 0.05
PET substrate	3.3 ± 0.03	--	0.33 ± 0.01

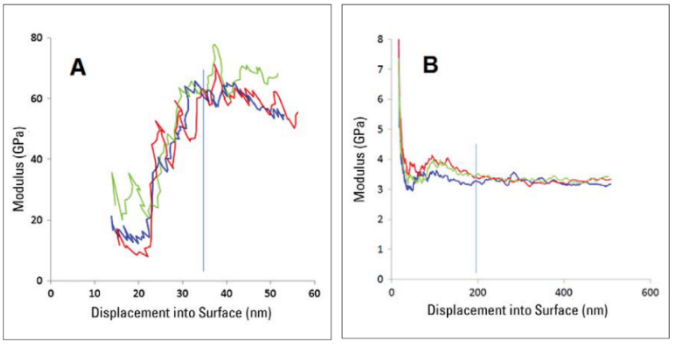

Figure 6. Young's modulus with increasing displacement into surface for (A) ITO thin film, and (B) PET substrate. The vertical straight lines indicate the depth beyond which the modulus is almost independent of displacement.

The flexural stress–strain curves for the different sample geometries are shown in Figure 7. The criterion for the optimum sample dimension is the ability to use the maximum ranges of the stress and strain possible, before the maximum load limit or maximum deflection, without slippage, is reached.

From Figure 7, it is evident that the 10mm x 5mm sample experiences the maximum stress for a particular strain. It also

requires almost 500mN, which is the maximum load possible in the T150 UTM. Hence, the maximum width for this specimen had to be restricted to about 5mm. When the width was reduced to 3mm, the stress reduced marginally. However, this situation is not optimum, because the sample reached regime III (Figure 5) at a lower load. When the length of the sample was increased from 10mm to 15mm, the drop in maximum stress was even more significant. It is evident from Figure 7 that increasing the length also adversely affects the strain at maximum stress, i.e. the sample starts to slip at a much lower strain. On the other hand, the 3-point bend setup was not designed to hold samples of lengths less than about 10mm. Thus, an optimum sample dimension of 10mm x 5mm was used for obtaining the results discussed below.

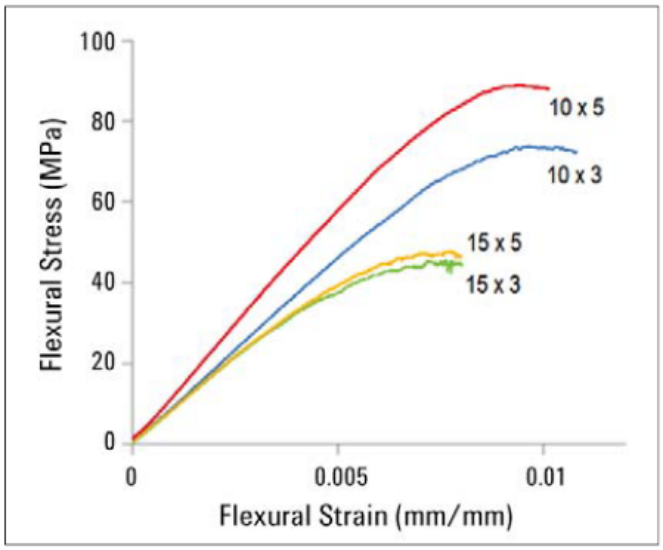

Figure 7. Flexural stress-strain curves for different geometries (length x width in mm).

As strain rate may affect the bending deformation and the dynamic stiffness measurement, it is important to determine a deflection rate that will provide fast results without compromising the quality of the results. The effect of changing deflection rate was studied by performing tests on samples of 10mm x 5mm geometry at different deflection rates ranging from 1µm/s to 50µm/s.

Figure 8A shows that the stress-strain curves are similar, except for the very slow deflection rate of 1µm/s. However, the deflection rates affected the dynamic stiffness measurements significantly, which can be seen in Figure 8B. These results indicate that at the lowest deflection rate (1µm/s), the noise in the quasi-static motion is significantly high and also affects the dynamic stiffness measurement. At deflection rates higher than 20µm/s, the quasi-static deflection interferes with the harmonic force and hence, the dynamic stiffness measurement becomes less accurate. At intermediate deflection rates, the dynamic stiffness measurements are consistent and the noise in the quasi-static stress-strain curves is also low. Hence, 20µm/s was chosen to be the optimum operating deflection rate. Note that these tests were carried out with the ITO film on the tensile side.

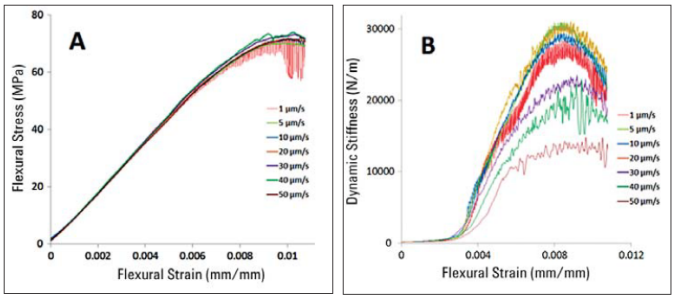

Figure 8. (A) Flexural stress-strain curves and (B) Dynamic Stiffness-strain curves at different deflection rates.

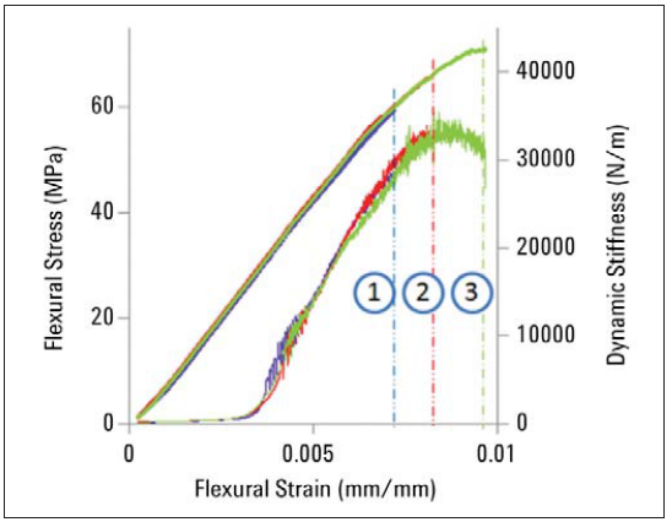

Figure 9. Combined plot of Flexural stress-strain and Dynamic Stiffness-strain for three different measurements up to different strains (marked 1, 2 and 3), tested with ITO film on the tensile side.

Figure 9 plots the flexural stress and corresponding dynamic stiffness for three different measurements, with ITO in the tensile configuration, up to different flexural strains, marked 1, 2 and 3. The flexural stress shows monotonous increase with increasing strain. However, the dynamic stiffness reveals new information with increasing strain. It is important to note here that the initial value of the dynamic stiffness matches exactly with the quasi-static stiffness value calculated from the initial

linear part of the load vs. deflection data. This agreement not only validates the dynamic stiffness calculations, but also provides an arguably more accurate means to calculate the elastic properties of flexible structures. It is expected in a bending experiment that the dynamic stiffness should increase with deflection. But, for the first time in this work, the evolution of dynamic stiffness value is measured continuously as a function of strain using the CDA in the T150 UTM. Beyond a strain of about 0.003, the rate of increase in dynamic stiffness changes suddenly. The exact reason behind this change is unclear at this moment but may be due to some changes in the interface between the ITO film and the PET substrate. Clearly, more work is needed to determine the physical nature of the interface.

The most interesting feature in the dynamic stiffness curves is observed at a higher strain of about 0.008, where the dynamic stiffness reaches a peak and then decreases. As the dynamic stiffness is related to the elastic deformation, a decrease in magnitude indicates a failure in the sample. In the beginning of this work, the understanding was that a failure in these flexible electronic samples due to bending is related to brittle fracture of the ceramic ITO film. To confirm the conjecture with the drop in dynamic stiffness values, tests were carried out (1) up to a strain below the peak, (2) up to the peak, and (3) beyond the peak of dynamic stiffness.

The ITO surfaces of all three samples were inspected in the optical microscope to observe the signs of brittle failure. The optical micrographs of the surfaces near the center of the samples are shown in Figure 10. Sample 1 (Figure 10A) shows no crack on the ITO surface. Sample 2 (Figure 10B), that was deformed until the highest dynamic stiffness, shows only a few cracks. Sample 3 (Figure 10C) was tested beyond the maximum stiffness and exhibits a higher concentration of cracks.

Figures 10B and 10C clearly show that the dynamic stiffness measurements were consistent with brittle cracking in the ITO thin film.

The cracks that form on the ITO are very fine and can barely be observed in the optical microscope. A plasma etch-based procedure has been reported[14] that highlights bending cracks in transparent films on plastic substrates. In this method, the polymer substrate is etched at locations where defects are present. This method facilitates clear identification of cracks in thin films. However, we did not opt for this method due to lack of necessary equipment. One sample that was deformed similarly to Sample 3 in Figure 9 was investigated using the SEM for characterizing the crack morphology. The crack was found to be very thin (10–20 nm in width), and ran straight through the ITO surface, with very small deviations, as shown in Figure 11.

Similar experiments were also performed with the ITO film on the compression side. The variations in flexural stress and

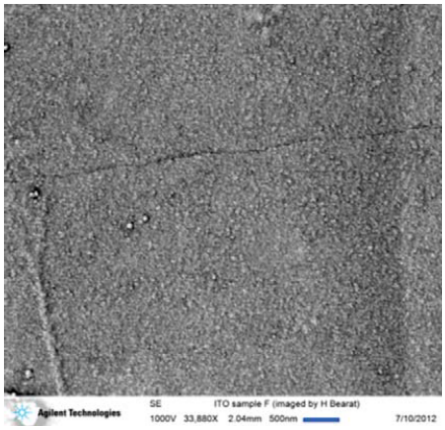

Figure 11. SEM image showing crack on ITO surface, due to 3 point bending in tensile mode.

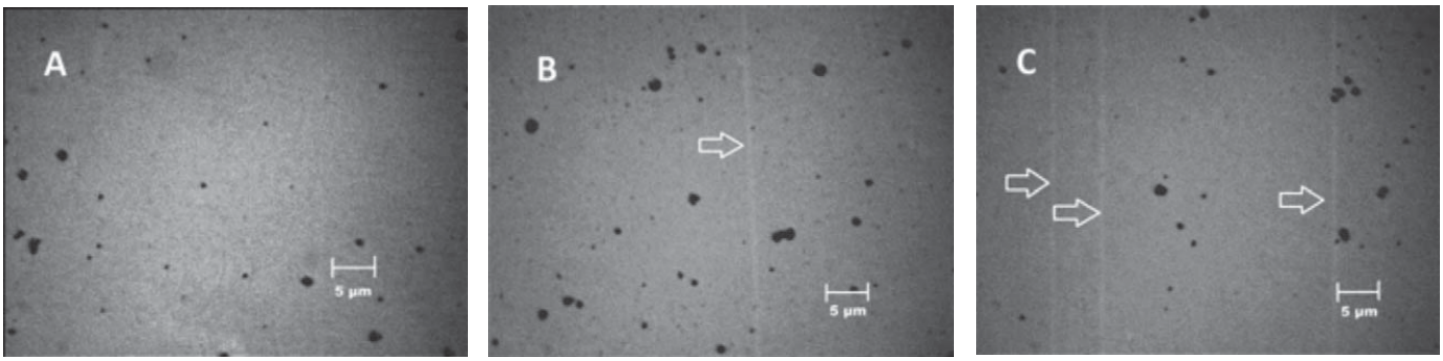

Figure 10. Optical micrographs of the ITO surface of (A) Sample 1, (B) Sample 2, and (C) Sample 3, showing cracks formed due to three point bending, with ITO film on the tensile side.

dynamic stiffness as a function of strain are shown in Figure 12. The dynamic stiffness measurements showed a similar trend, but beyond the peak, there were oscillations in the data along with the drop in dynamic stiffness. These oscillations indicate more drastic failure events that occur in the brittle ITO film.

The optical micrographs of the ITO surface, from the three samples characterized with the ITO film on compression, are shown in Figure 13. In contrast to Figure 10, the cracks observed in the samples tested up to the peak (Figure 13B) and beyond the peak (Figure 13C) of dynamic stiffness are more prominent, indicating severe cracking in the ITO film.

When a sample tested in compression mode was imaged in the SEM (Figure 14), interesting features of the cracks were observed. The actual cracks were very thin, of the order of a few nanometers, but the sides of the cracks show a deformation that occurred during testing. The deformed zone was of the order of 0.5µm on each side of the cracks, enabling the observation of these cracks in the optical microscope. The

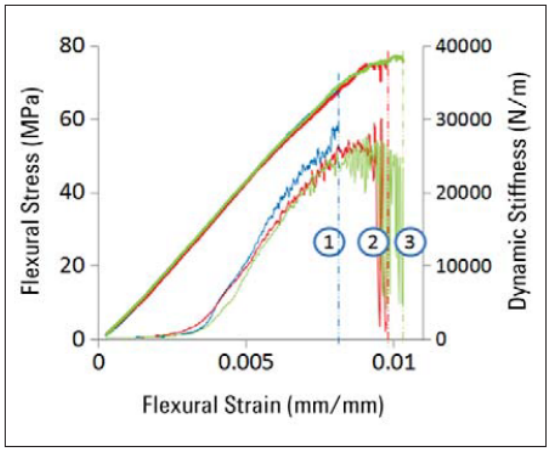

Figure 12. Combined plot of Flexural stress-strain and Dynamic Stiffness-strain for three different measurements up to different strains (marked 1, 2 and 3), tested with ITO film on the compressive side.

deformations on the sides of the cracks are more prominent when observed in the unique topographical mode, available in the Agilent 8500 FE-SEM. The ITO film buckles and delaminates

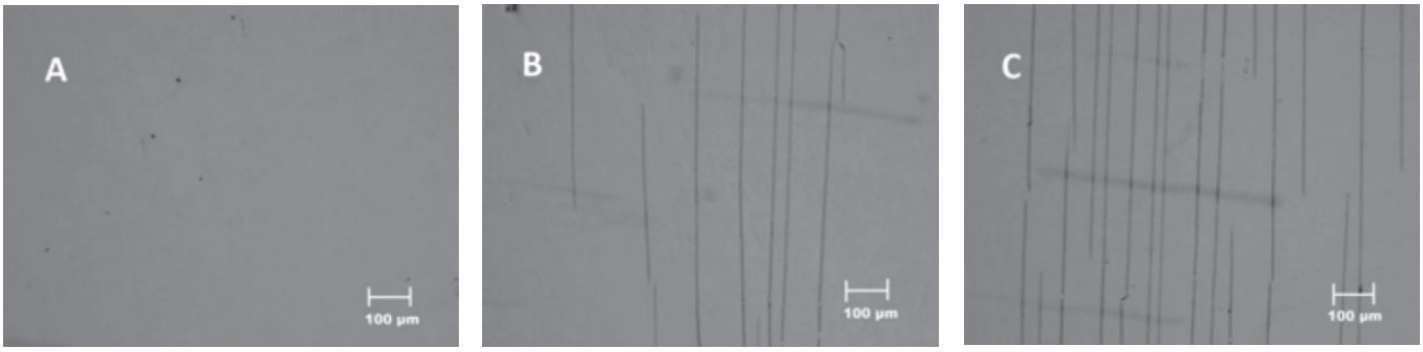

Figure 13. Optical micrographs of ITO surface of (A) Sample 1, (B) Sample 2, and (C) Sample 3, showing cracks formed due to three point bending, with ITO film on the compressive side. As these images are taken at a lower magnification, scratches on the PET surface below are seen as dark horizontal lines.

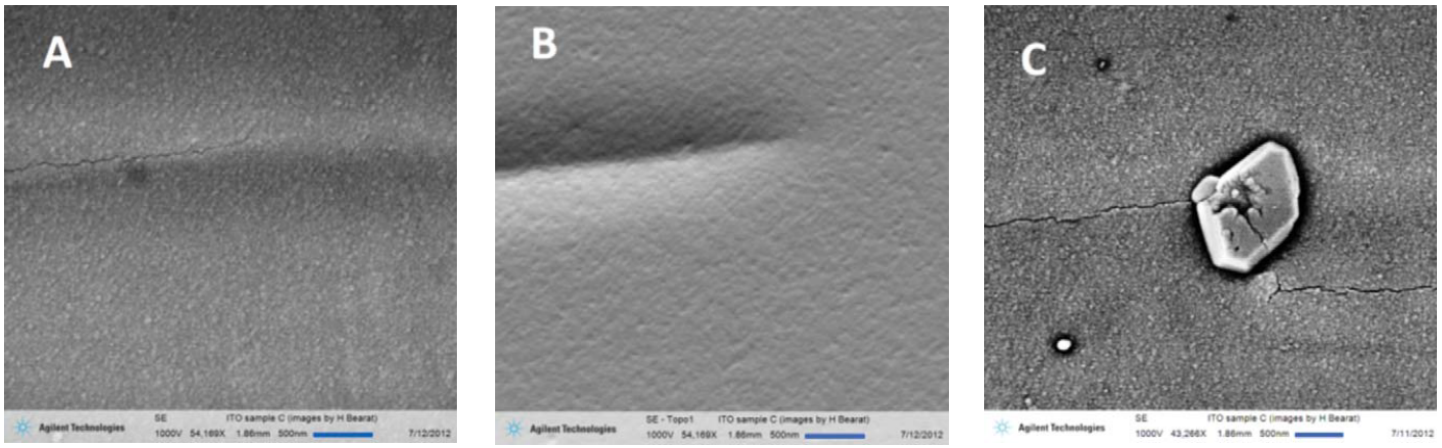

Figure 14. SEM image of a crack on ITO surface imaged with secondary electrons in (A) normal mode, and (B) topographic mode, showing a thin crack with a deformed zone on either side. (C) SEM image showing a crack passing through a crystal on the ITO surface.

while it is on the compression side of the flexing PET substrate. Upon large deformation, these buckled regions reach the critical radius of curvature for the ITO film to form cracks, which propagate across the sample.

The buckles in the ITO film causes random initiation of cracks that can be linked to the oscillations observed in the dynamic stiffness (Figure 12). Previous FEM analysis of a similar 3-point bend setup[15], have also shown that the middle section across the width of the sample experiences high stress concentrations. This can be a possible explanation for the cracks, observed to start/end in the middle of the film (Figures 14A and 14B). The SEM observations also confirmed that the surface spots that were observed in the optical microscope were actually crystalline regions on the surface of the ITO film (Figure 14C). These regions were about 1µm in diameter, and most likely small crystals formed during processing of the ITO film. Some of these particles in the surface were on the path of crack propagation. Depending on the crystallography, the cracks were either deflected around or pass across these particles.

To further validate our conclusion that the observed drop in the dynamic stiffness is indeed related to brittle failure of the ITO film, tests were carried out on samples where the ITO was completely etched out, leaving only the PET substrate. The PET substrates were tested similar to the prior samples and the dynamic stiffness response was analyzed.

Figure 15A shows the flexural stress-strain behavior of the samples containing only PET. For the ease of comparison, the results for samples with ITO film are also plotted in the same graph. Figure 15B shows the corresponding change in dynamic stiffness. Although the PET samples were deformed up to a larger strain without slippage in the 3-point bend fixture, the flexural stress for the ITO-PET samples is higher for any particular strain. The results also show that the drop in dynamic stiffness that occurred due to inception of brittle failure was not observed in the PET samples. This is a valid proof that the CDA can be used successfully to determine failure initiation in brittle thin films in flexible electronic structures. Some etched samples were also characterized, keeping the etched surface on the compressive side. The results were very similar to those of the tensile etched samples, further supporting our explanations.

As mentioned earlier, failure in the thin inorganic film on flexible substrates adversely affects the performance of the electronic device, which should deteriorate over time with cyclic

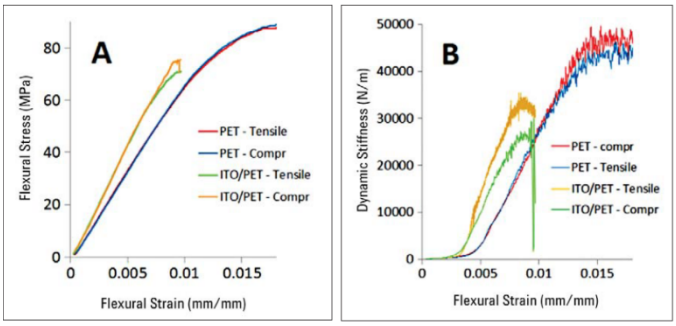

Figure 15. (A) Flexural stress-strain curves of ITO/PET and PET-only samples tested in tensile and compression modes; (B) Dynamic Stiffness-strain curves of ITO/PET and PET-only samples tested in tensile and compression modes.

deformation of the thin film. The severity of this fatigue effect was studied by performing cyclic bend tests for up to 200 cycles, keeping the ITO on the tensile side. Electrical resistance of each sample was measured before and after the tests to study the degradation of the ITO thin film. Because the 100 and 200 cycle experiments took a long time, resistance measurements immediately after the test were not possible. Hence, for all samples, resistance measurements were also carried out after aging the samples for a period greater than 34 hours after the test. The normalized change in resistance is calculated as:

$$\Delta R = (R_f - R_i)/R_i \qquad (6)$$

where R_f is the resistance measured after the test, and R_i is the resistance measured before the test. Figure 16 shows the plot of normalized change in resistance with number of cycles.

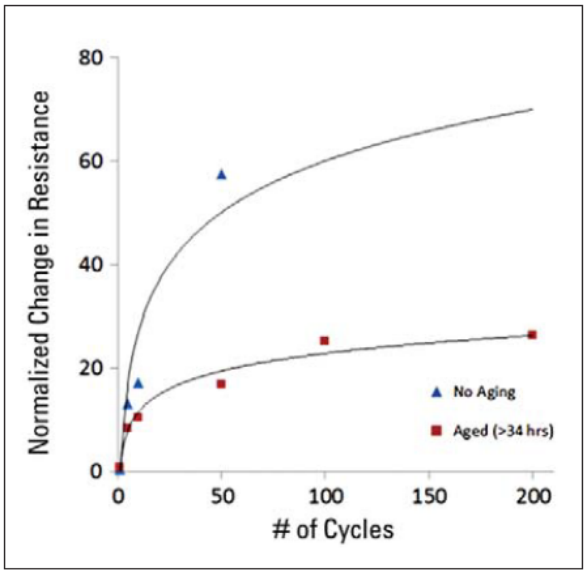

Figure 16. Plot of Normalized change in resistance - number of cycles for samples without aging, and after about 34 hours of aging.

The results indicate that the resistance change follows a logarithmic trend with increase in number of cycles. The measurements for samples after more than 34 hours of aging indicate a significant drop in the resistance, which may have been caused due to stress relaxation and closure of the cracks. In-situ electrical measurements are required to understand the exact mechanism of fatigue in these flexible structures.

Summary and Conclusions

The KLA T150 UTM has been successfully utilized to characterize nano/micro-mechanical failure in inorganic thin films on flexible substrates; in this work, Indium Tin Oxide (ITO) coated on Polyethylene Terephthalate (PET) substrate. The novel test methodologies developed for three point bending combine the capability of measuring sample dynamic response continuously with quasi-static deformation and use it to study small changes in deformation mechanism and brittle failure initiation. The load and displacement capabilities of the T150 have been shown to be adequate once critical experimental parameters such as sample geometry and bending deflection rate are optimized. The measurement of the evolution of dynamic stiffness as a function of flexural strain was unprecedented and successful in determining failure initiation in a brittle ITO film on a flexible PET substrate. Compared to tensile mode, failure of the ITO film in compression mode was more drastic. Increase in electrical resistance upon cyclic bending show the importance of understanding mechanical damage propagation and its effect on functional behavior of flexible electronic structures. This work combined the results from the T150 with thin film modulus measurements from the Nano Indenter G200 and high resolution SEM micrographs, emphasizing the important role the nano measurement solutions could play for research and development of flexible electronics.

References

1. J.A. Rogers, T. Someya and Y.G. Huang, “Materials and mechanics for stretchable electronics,” Science 327, 1603–1607 (2010).
2. J. Hay, “Tensile Testing of Basalt fibers using a T150 UTM”, KLA Application note, 2009.
3. J. Swindeman, “Continuous Dynamic Analysis and Quasi-static measurement of spider silks”, KLA Application note, 2009.
4. J. Hay, “Quasi-static and Dynamic properties of technical fibers”. KLA Application note, 2010.
5. S. Basu, “Tensile test of copper fibers in conformance with ASTM C1557 using the T150 UTM”. KLA Application note, 2011.
6. S. Chan, H. Yang, F. Ko, C. Ayranci and S. Basu, “Tensile Stress-Strain response of small-diameter electrospun fibers,” KLA Application note, 2012.
7. S. Basu, “Tensile deformation of fibers used in the Textile industry,” KLA Application note, 2012.
8. http://en.wikipedia.org/wiki/Three_point_flexural_test.
9. Z. Suo, E.Y. Ma, H. Gleskova and S. Wagner, “Mechanics of rollable and foldable film-on-foil electronics,” Applied Physics Letters, 74, 1177–1179 (1999).
10. http://sigmaaldrich.com/materials-science/material-science-products.html?TablePage=9548901.
11. J. Hay and B. Crawford, “Measuring substrate independent modulus of thin films,” Journal of Materials Research, vol. 26, pp. 727–738, 2011.
12. K.Y. Lee, H.J. Shin, D.C. Han, S. Son, S.W. Kim, Y.S. Lee and D.K. Lee, “Fabrication of transparent semiconducting Indium Zinc Tin oxide thin films and its wet chemical etching characteristics in Hydrochloric acid,” Molecular Crystals and Liquid Crystals, vol. 532, pp.141/[557]–147/[563], 2010.
13. D.-H. Kim, H.-K. Yoon, D.-H. Shin, R.I. Murakami, “Mechanical properties of ITO/PET thin film deposited by DC MG method,” Proceedings of the International Symposium on Electronics Materials and Packaging, pp. 174–178, 2005.
14. S. Grego, J. Lewis, E. Vick and D. Temple, “A method to evaluate mechanical performance of thin transparent films for flexible displays,” Thin Solid Films, vol. 515, pp. 4745–4752, 2007.
15. K. Alzoubi, M.M. Hamasha, S. Lu and B. Sammakia, “Bending fatigue study of sputtered ITO on flexible substrate,” Journal of Display Technology, vol. 7, no. 11, pp. 593–600, 2011.

KLA Corporation
One Technology Drive
Milpitas, CA 95035
Printed in the USA
Rev 2 2020-09-14